XXXVI Ibero-Latin American
Congress on Computational
Methods in Engineering
CILAMCE
Rio de Janeiro, 22-25 Nov 2015

NONLINEAR TRANSIENT ANALYSIS OF PLANAR STEEL FRAMES WITH SEMI-RIGID CONNECTIONS

Everton A. P. Batelo

Andréa R. D. Silva

Ricardo A. M. Silveira

everton.batelo@gmail.com

andreadiassilva@yahoo.com.br

ricardo@em.ufop.br

Graduate Program in Civil Engineering (PROPEC), Department of Civil Engineering (Deciv), Federal University of Ouro Preto (UFOP)

Campus Universitário, Morro do Cruzeiro, 35400-000, Ouro Preto, Minas Gerais, Brazil

Abstract. *For all steel structural construction that involves one or more floors, the use of beam-column or even column-base connections is inherent. Due to their importance, these connections are, in steel structures, economically and structurally significant. Also in some situations, these steel buildings are subjected to a dynamic load level that can cause permanent deformation and localized damage in the structure, and this may lead to its partial or total collapse. To obtain a more realistic prediction of the behavior of steel structures, the flexibility of the connection between the members should be considered in the analysis. This work aims to evaluate the nonlinear behavior of steel frames structures under dynamic loads, showing the influence of the semi-rigid connections in response of the structure, and also exploring the structural hysteretic damping. The modeling strategy used is based on the Finite Element Method application, and the transient nonlinear solver adopted combines the methods of Newmark and Newton-Raphson. At the end of the work is carried out a numerical study of a four-bay five-story planar steel frame with beam-column semi-rigid joints. From the analysis, it will be possible note that the flexible connections flexibility has significant influence on variation of the natural frequencies, particularly on the lower frequencies and on the frame nonlinear behavior.*

Keywords: *Steel frames, Geometric nonlinearity, Semi-rigid connection, Hysteretic damping*

1 INTRODUCTION

Multi-story steel buildings gained increasing space in the civil construction sector, since they are economical and safe solutions for the most varied types of projects. The steel frames in general are slim, efficient and quick to assemble. A careful structural analysis of such slim structures is of fundamental importance because it results in a safe and efficient building along the entire its service life.

In steel structural construction, the use of beam-column or even column-base connections is inherent. Due to their importance, these connections are, in steel structures, economically and structurally significant. Analysis and project enhancement for structures with semi-rigid connections is cost effective, carrying significant implications for manufacturers and assemblers of these steel structures. It is important, then, that the engineer has a good project understanding of connection behavior. For this reason, diverse studies are under development and modern standards (NBR 8800, 2008; AISC, 2010; Eurocode, 2005) already include procedures that define stiffness as well as strength for semi-rigid connections for computational analysis programs and steel structure projects.

The random motion of the structure base, as occurs in case of structures subjected to earthquakes, is characterized by a dynamic action. Therefore, the structural response of buildings to earthquakes is a transient phenomenon. Although there is a low seismicity in Brazil, this action cannot always be ignored, even for small buildings (Lima and Santos, 2008).

In steel structural construction, the nonlinear behavior of beam-column connections significantly affects the dynamic response under earthquakes since connection regions are one of the primary sources of hysteretic damping.

Researchers who have numerically investigated the behavior of steel structures with semi-rigid connections submitted to dynamic situations include the following: Valipour and Bradford (2012); Chan and Ho (1994); Lui and Lopes (1997); Xu and Zhang (2001); Sophianopoulos (2003); Galvão *et al*. (2010); Vimonsatit *et al*. (2012); Nguyen (2010); Nguyen and Kim (2011); Attarnejad and Pirmoz (2014); Aristizabal-Ochoa (2015).

The cyclic responses of semi-rigid connections have also been experimentally evaluated. In such studies as Bernuzzi *et al*. (1996), Calado (2003), and Shi *et al*. (2007), tests were performed with specific types of connections and mathematical models were proposed to represent the resulting behavior.

This study considers the geometric nonlinear effects and the semi-rigid connections between the structural elements. The computational system for advanced structural analysis CS-ASA (Silva, 2009) was used in this work. The main application of this tool is the nonlinear static and dynamic analysis of planar steel structures. Small interventions were performed in CS-ASA system in order to enable this research for include real ground motions.

2 SEMI-RIGID CONNECTIONS

Figure 1 illustrates the typical behavior of three types of semi-rigid connections: the flush end plate, top and seat angle, and single web angle. The figure demonstrates the variation of the rotation ϕ_c, which corresponds to the relative rotation between the interconnected elements, with an applied moment. Notice that the connections, when submitted to bending, develop a nonlinear behavior.

The connection stiffness, denoted here as S_c, is determined by experimental tests; it describes the performance of the connection during the loading process. Mathematically, it represents the inclination of the tangent to the moment-rotation curve (Fig. 1).

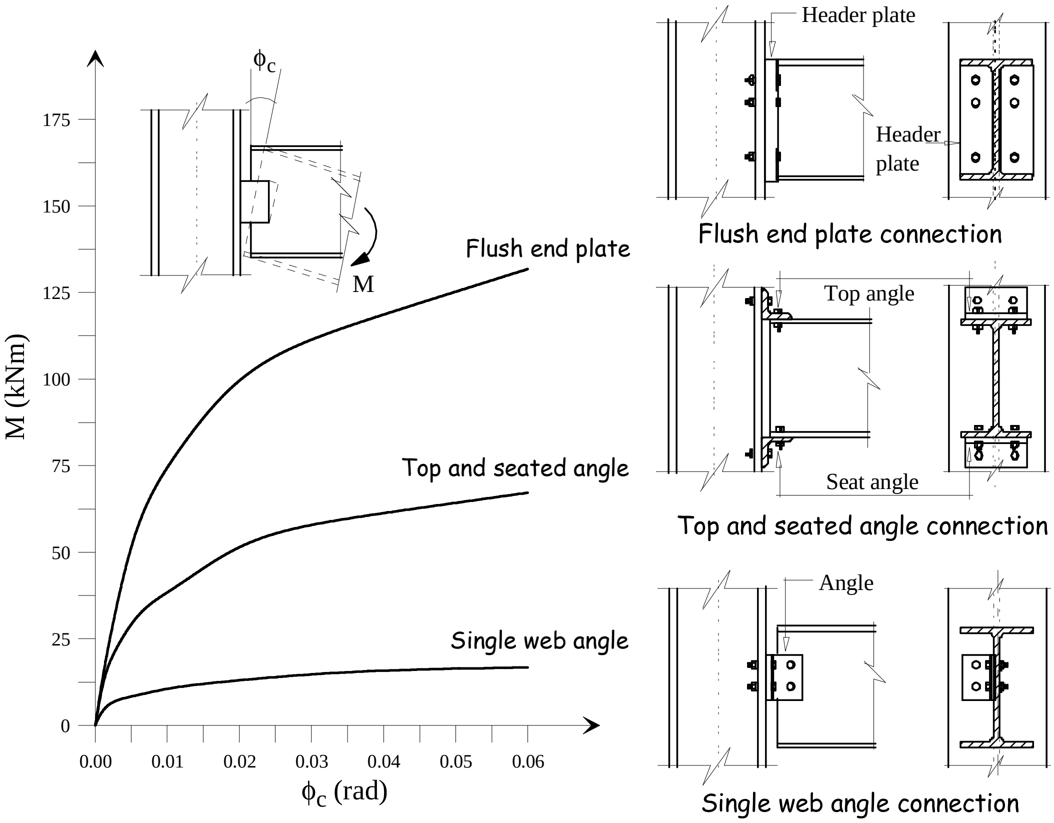

Figure 1. Moment-rotation curves of three types of connections under monotonic loading (Silva, 2009)

The stiffness intensity does not determine whether a connection will behave in a rigid or flexible manner. This behavior can only be verified by using a parameter that relates the connection's stiffness to the bending stiffness (*EI*) of the element to which it is connected. Cunningham (1990) proposed adopting a fixed factor for rigidity, $\gamma = (1 + 3EI/(S_cL))^{-1}$, in which L represents the element's length. Cunningham proposed this to provide a better understanding of the rotational behavior of the connection. The extreme values that the fixed factor assumes are 0 and 1. For a perfectly hinged connection, the rigidity is null (γ = 0). However, for an ideally rigid connection, the fixed factor has a value of 1, since its stiffness is extremely high ($S_c \rightarrow \infty$).

The connection stiffness can be calculated using the equation:

$$S_c = \frac{dM}{d\phi_c} \tag{1}$$

where M is the bending moment acting on the connection and ϕ_c is its rotational deformation.

Incorporation of moment-rotation curves in structural analysis provides more precise results than those obtained through conventional analysis. In conventional analysis, the connections are considered either rigid or hinged. Such curves can generally be written by using one of the following expressions:

$$M = f\left(\phi_c\right)$$
$$\phi_c = g\left(M\right) \tag{2}$$

which relate the moment to the rotation with the mathematical expressions *f* and g, which usually depend on the geometry and disposition of the connecting components and the curve adjustment parameters.

The mathematical models should provide a smooth moment-rotation curve with the first derivative positive and representing various types of connections. For a linear connection model only one parameter defining the joint stiffness is necessary. In this case, the moment-rotation relationship can be written as:

$$M = S_{cini}\phi_c \tag{3}$$

in which S_{cini} represents the initial stiffness, which is determined by the initial stage of loading. This is the simplest model and has great use in the initial development stages of analysis methods for semi-rigid connections. For large displacements, however, it is not abundantly precise. Its utilization is more appropriate for small displacements, such as the linear analyses of vibrations and (Chan and Chui, 2000).

This work uses the four-parameter potential model proposed by Richard and Abbott (1975) for simulate the nonlinear behavior of connections The model describe the connection behavior according to the relationship:

$$M = \frac{\left(S_{cini} - R_p\right)\left|\phi_c\right|}{\left[1 + \left|\left(S_{cini} - R_p\right)\left|\phi_c\right| / M_o\right|^n\right]^{1/n}} + R_p\left|\phi_c\right| \tag{4}$$

where *M* is the moment in the connection, R_p is the strain-hardening stiffness when ϕ_c tends towards infinity; *n* is a parameter that defines the sharpness of the curve, and M_o is the reference moment.

A study made by Kishi *et al*. (2004) demonstrated that this model is effective and necessary to pre-establish the behavior of an end plate connection. It is worth mentioning, however, that this type of function can be applied to any type of connection. To do this, it is sufficient to either experimentally or numerically evaluate the four parameters necessary to represent it. With this model, three others can be obtained: linear ($R_p \approx S_{cini}$), bilinear ($n \to \infty$), and ignoring the effect of the strain-hardening stiffness, which produces a three-parameter potential model, as presented by Kishi and Chen (1986). Therefore, it must be emphasized that the stiffness of the connection is calculated by using Eq. (1), with *M* described by Eq. (4).

2.1 Behavior of semi-rigid connection under cyclic loading

When submitted to repetitive and alternate actions, semi-rigid connections also develop an inelastic behavior. The typical aspects of such behavior are illustrated in Fig. 2. Some phases along the trajectory can be clarified in accordance with this figure. The *0A* part describes the connection's behavior during the initial loading process of the structure. When an inversion occurs in the direction solicited, the process of unloading is characterized. Therefore, the intensity is diminished of the bending moment that acts on the connections.

The arrows establish the direction of the paths, indicating moment variation during the analysis. The *AB* and *CD* paths in the figure exhibit such a situation.

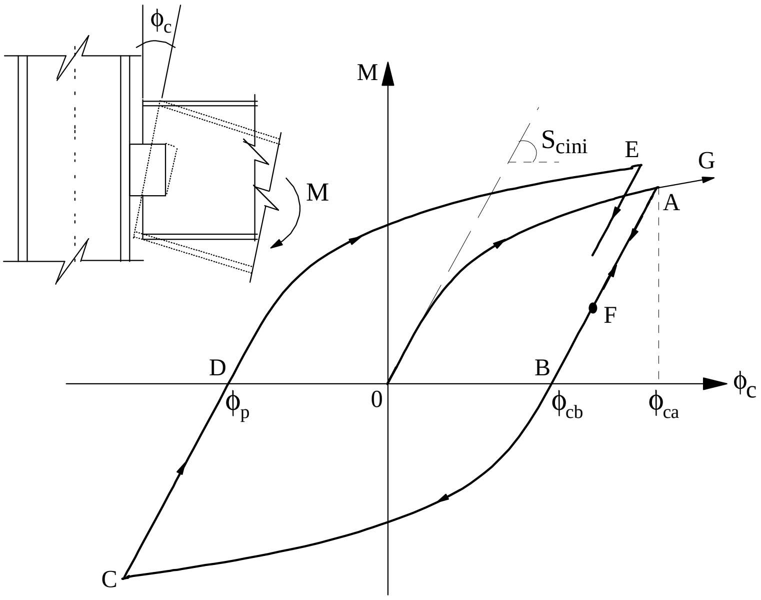

Figure 2. Connection behavior under cyclic loading (Silva, 2009)

The inelastic behavior of the semi-rigid connections when submitted to cyclical loads has been simulated by the independent hardening technique. The model is used to evaluate the connection stiffness in the loading and unloading stages.

The following steps describe the procedure used to develop an algorithm that simulates the hysteretic behavior illustrated in Fig. 2. Under loading conditions, the trajectory (indicated by the continuous lines in Fig. 3a) begins at a point along the abscissas axis whose coordinates correspond to ϕ_p, the last permanent residual rotation. At *0A*, the initial loading phase, $\phi_p = 0$. As mentioned above, this rotation is determined after the complete unloading phase. The bending moment *M* at any position of this trajectory that begins at *D* can generally be calculated as follows:

$$M = f\left(\phi_c - \phi_p\right) \tag{5}$$

where the expression f is defined in accordance with a mathematical model that describes the nonlinear moment-rotation behavior of the connection when submitted to a monotonic load. While the connection stiffness is given by:

$$S_c = \left.\frac{dM}{d\phi_c}\right|_{\phi_c=\left(\phi_c-\phi_p\right)} \tag{6}$$

Note that the loading phase is characterized by an increase in the bending moment, ΔM, between the instants of time: t (prior) and $t + \Delta t$ (actual). Besides this, the sign of ΔM is always equal to the involved bending moment, *M*. Therefore, the loading condition can be verified if the $M{\cdot}\Delta M > 0$ relationship is satisfied.

What is considered in the unloading process is a linear moment-rotation curve with an inclination equal to the initial stiffness of the connection. Figure 3b exhibits the regions where the unloading occurs. A solid line is used to indicate this. To obtain the moment-rotation equations at this phase, consider the strip *AB* of the hysteresis cycle represented in Fig. 3. As the straight line passes through the point $A(\phi_{ca}; M_a)$ and has a known inclination of S_{cini}, its equation is defined as:

$$M = M_a - S_{Cini}\left(\phi_{ca} - \phi_c\right) \tag{7}$$

where M_a is the moment at which unloading occurs. This variable, referred to as the reverse moment, is encountered using Eq. (5) for $\phi_c = \phi_{ca}$.

It is easy to see that, during the unloading process, the $M \cdot \Delta M < 0$ relationship is obeyed. However, in some case additional clarifications are necessary. Consider again Fig. 2. If the connection is being unloaded from *A* to *F* and begins the loading process before the unloading has been completed, the moment-rotation behavior of this element will follow the *FA* trajectory until it reaches the last reverse moment encountered. At this point in time, the loading process follows the original moment-rotation curve obtained considering the last permanent rotation ϕ_p encountered.

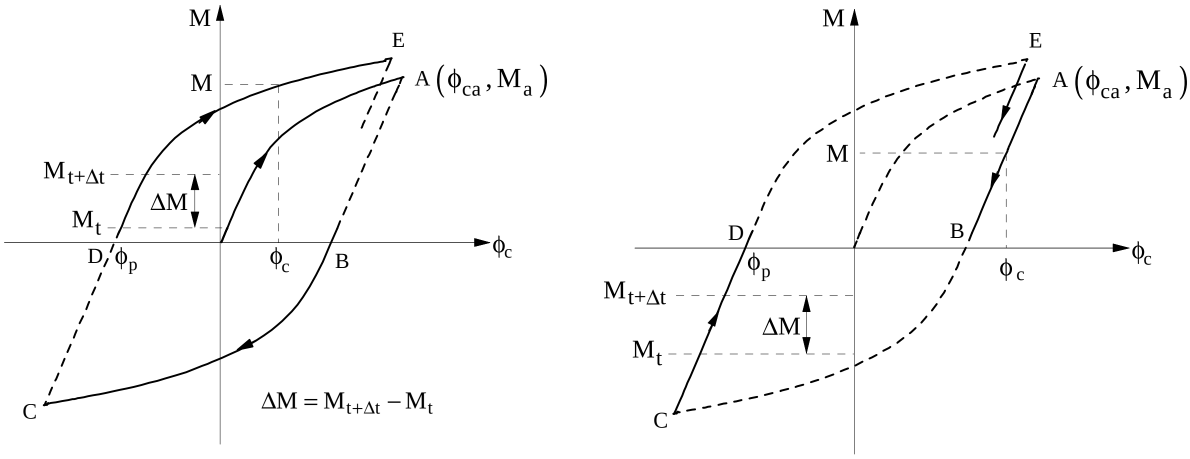

(a) Loading (b) Unloading

Figure 3. Connection behavior under cyclic loading (Silva, 2009)

In computing the independent hardening model, the ϕ_p rotation should be stored after each complete unloading situation. This is true also for the reverse moment M_a, every time an alteration is detected in the sign of the moment increment ΔM. In addition, the intervals between the two successive time instants should be small so that these variables can be defined with adequate precision.

3 THE SEMI-RIGID FINITE ELEMENT

The most common approximation method for modeling a connection in structural analysis programs uses springs positioned at the extremities of the finite element. Figure 4 shows the planar beam-column element, with node points *i* and *j*, that was used in this work to model the structural systems. The two springs are physically fixed at the extremities of the beam-column element, respecting the equilibrium and compatibility conditions. They permit the connections' degree of freedom to be incorporated into the relationship of the tangent stiffness of the beam-column element. Only the connection's rotational deformation due to bending is considered.

The presence of springs introduces relative rotations in the nodes at the extremities of the element. These rotations modify the equations that describe the nonlinear behavior of the ideally rigid structural system. This section proposes a procedure to modify the matrix equations so as to introduce the effects, on the beam-column element, of the connection's flexibility.

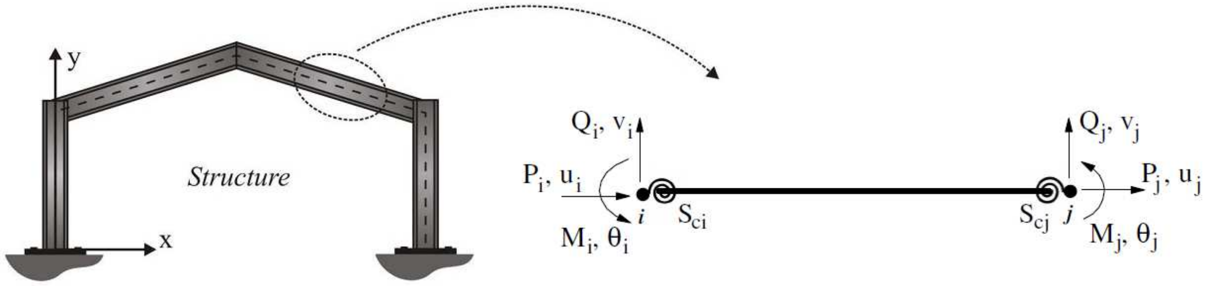

Figure 4. Beam-column element with semi-rigid connections

Figure 5 shows a deformed configuration of the finite element. Also exhibited here are the internal forces and deformations in the springs of the connection. S_{ci} and S_{cj} denote the stiffness of the spring elements. The connections can have distinct behaviors; that is, they can be characterized by different moment-rotation curves (Eq. 6). The connection's relative rotation, ϕ_c, is defined as the difference between the rotational angles of the side connected with the global node of the element, θ_c, and those connected to the beam-column element, θ_b. Considering this, it is possible, using Eq. (6) and establishing the moment equilibrium of the spring elements, to come up with the following relationships:

$$\begin{Bmatrix} \Delta M_{ci} \\ \Delta M_{bi} \end{Bmatrix} = \begin{bmatrix} S_{ci} & -S_{ci} \\ -S_{ci} & S_{ci} \end{bmatrix} \begin{Bmatrix} \Delta\theta_{ci} \\ \Delta\theta_{bi} \end{Bmatrix} \tag{8}$$

$$\begin{Bmatrix} \Delta M_{cj} \\ \Delta M_{bj} \end{Bmatrix} = \begin{bmatrix} S_{cj} & -S_{cj} \\ -S_{cj} & S_{cj} \end{bmatrix} \begin{Bmatrix} \Delta\theta_{cj} \\ \Delta\theta_{bj} \end{Bmatrix} \tag{9}$$

where M_c and M_b are, respectively, the bending moments acting on the spring elements and those acting on the beam-column element; the subscripts i and j refer to the element's extremities.

When spring connections are added to the element's extremities, the effect induced by connection flexibility should be accounted for by modifying the element stiffness matrix. How the matrix is modified depends on the finite element formulation adopted. Herein, the spring elements simulating the connection's flexibility have null lengths and for the element's internal sections.

Assuming that the loads are only applied at the global nodes of the element (see Fig. 5), the internal M_{bi} and M_{bj} moments are equal to zero, and the following moment-rotation equilibrium relationship can be achieved (Silva,2009):

$$\begin{Bmatrix} \Delta M_{ci} \\ \Delta M_{cj} \end{Bmatrix} = \left(\begin{bmatrix} S_{ci} & 0 \\ 0 & S_{cj} \end{bmatrix} - \frac{1}{\beta} \begin{bmatrix} S_{ci} & 0 \\ 0 & S_{cj} \end{bmatrix} \begin{bmatrix} S_{cj} + k_{(6,6)} & -k_{(3,6)} \\ -k_{(6,3)} & S_{ci} + k_{(3,3)} \end{bmatrix} \begin{bmatrix} S_{ci} & 0 \\ 0 & S_{cj} \end{bmatrix} \right) \begin{Bmatrix} \Delta\theta_{ci} \\ \Delta\theta_{cj} \end{Bmatrix} \tag{10}$$

in which $\beta = \left(S_{ci} + k_{(3,3)}\right)\left(S_{cj} + k_{(6,6)}\right) - k_{(6,3)}k_{(3,6)}$.

Figures 4 and 5 show that $M_i = M_{ci}$ and $M_j = M_{cj}$. As such, the relationship between the shearing forces and the bending moments, obtained by the equilibrium force and moment ($\Sigma F_y = 0$ and, for example, $\Sigma M_i = 0$), can be written in an incremental matrix, as follows:

$$\begin{Bmatrix} \Delta Q_i \\ \Delta M_i \\ \Delta Q_j \\ \Delta M_j \end{Bmatrix} = \begin{bmatrix} 1/L & 1/L \\ 1 & 0 \\ -1/L & -1/L \\ 0 & 1 \end{bmatrix} \begin{Bmatrix} \Delta M_{ci} \\ \Delta M_{cj} \end{Bmatrix} \tag{11}$$

with ΔM_i and ΔM_j being the incremental nodal moments; ΔQ_i and ΔQ_j being the incremental shearing forces; and L being the element length in the configuration of the equilibrium t.

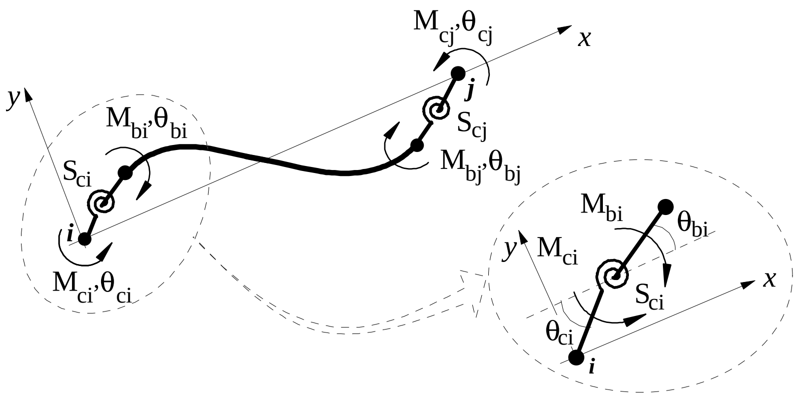

Figure 5. Deformed configuration and spring element degree of freedom (Silva, 2009)

Observing Fig. 6, it is possible to establish the relationship:

$$\begin{Bmatrix} \Delta\theta_{ci} \\ \Delta\theta_{cj} \end{Bmatrix} = \begin{bmatrix} 1/L & 1 & -1/L & 0 \\ 1/L & 0 & -1/L & 1 \end{bmatrix} \begin{Bmatrix} \Delta v_i \\ \Delta\theta_i \\ \Delta v_j \\ \Delta\theta_j \end{Bmatrix} \tag{12}$$

The semi-rigid element stiffness matrix may then be obtained in which its components collectively consider the connection flexibility effect and the geometric nonlinear effects. This is done by substituting (10) into (11), using (12), and performing all the necessary operations. Using these new terms in the complete matrix (6x6 order) of the conventional beam-column element, this element's stiffness matrix is finally achieved in the local system of coordinates. In this formulation, the relationship between the axial forces P_i and P_j, and the displacement nodes suffer no alterations when considering the connection flexibility effects. The transformation of the internal force vector and the stiffness matrix for the global system of coordinates is carried out following the usual procedure.

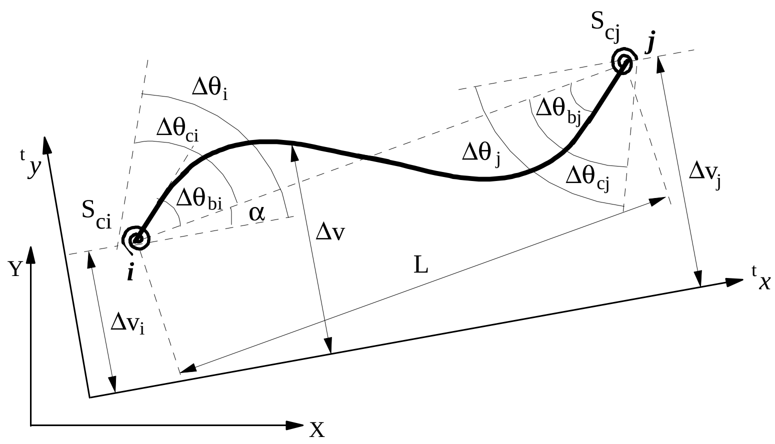

Figure 6. Nodal displacements of the semi-rigid beam-column element (Silva, 2009)

3.1 Semi-rigid element mass matrix

The consistent mass matrix for the conventional beam-column element is defined as (Kishi and Chen, 1986):

$$\mathbf{M}_e = \int_{{}^tV} \mathbf{H}^T \rho \mathbf{H} dV \tag{13}$$

where **H** is the interpolation functions matrix, while ρ, as already defined, is the volumetric mass of the element.

The function that describes the transversal displacement field v for the beam element can be written, in an incremental form, using the following matrix relationship:

$$\Delta v(x) = \left[H_1^2 H_2 L \quad -H_2^2 H_1 L \right] \begin{Bmatrix} \Delta\theta_{bi} \\ \Delta\theta_{bj} \end{Bmatrix} + \left[(3-2H_1) H_1 \quad (3-2H_2) H_2 \right] \begin{Bmatrix} \Delta v_i \\ \Delta v_j \end{Bmatrix} \tag{14}$$

where Δv_i and Δv_j are the incremental vertical displacements of, respectively, the nodes *i* and *j*, and $\Delta\theta_{bi}$ and $\Delta\theta_{bj}$ are the rotations of these same nodes, as shown in Fig. 6. In addition, $H1 = 1 - x/L$ and $H2 = x/L$.

To introduce the connection's flexibility effect into the previous function and thereby obtain the desired mass matrix, the beam-column nodal rotations are related to the rotations at the ends of the element with semi-rigid connections. The equation that describes such a relationship is:

$$\begin{Bmatrix} \Delta\theta_{bi} \\ \Delta\theta_{bj} \end{Bmatrix} = \begin{bmatrix} S_{ci} + \frac{4EI}{L} & \frac{2EI}{L} \\ \frac{2EI}{L} & S_{cj} + \frac{4EI}{L} \end{bmatrix}^{-1} \begin{bmatrix} S_{ci} & 0 \\ 0 & S_{cj} \end{bmatrix} \begin{Bmatrix} \Delta\theta_{ci} \\ \Delta\theta_{cj} \end{Bmatrix} \tag{15}$$

where *EI* is the flexural rigidity and L is the length of the element.

Substituting Eq. (13) into Eq. (15) and using (14), the function is encountered that describes the transversal displacement field for a beam with semi-rigid connections, i.e.:

$$\Delta v(x) = \mathbf{H}^* \left\{ \Delta v_i \quad \Delta\theta_i \quad \Delta v_j \quad \Delta\theta_j \right\}^T \tag{16}$$

in which,

$$\mathbf{H}^* = \left[H_1^2 H_2 L \quad -H_2^2 H_1 L \right] \begin{bmatrix} S_{ci} + \frac{4EI}{L} & \frac{2EI}{L} \\ \frac{2EI}{L} & S_{cj} + \frac{4EI}{L} \end{bmatrix}^{-1} \begin{bmatrix} S_{ci} & 0 \\ 0 & S_{cj} \end{bmatrix} \begin{bmatrix} 1/L & 1 & -1/L & 0 \\ 1/L & 0 & -1/L & 1 \end{bmatrix} + \left[(3-2H_1)H_1 \quad 0 \quad (3-2H_2)H_2 \quad 0 \right] \tag{17}$$

is the matrix that contains the semi-rigid connection's interpolation functions.

The mass matrix components that are influenced by the connection's stiffness are encountered using this new **H*** matrix, instead of the **H** in Eq. (13). The other terms are identical to the mass matrix developed for the conventional beam-column element whose connections are supposedly ideally rigid (Silva, 2009).

4 SOLUTION FOR THE TRANSIENT PROBLEM

The equilibrium equation that governs the nonlinear dynamic response of a structural system can be obtained using the Virtual Displacement Principle (VDP), considering that, besides the stresses induced by structural deformation, the system is also submitted to inertial and damping forces.

To determine the equilibrium configuration of the structure in state $t+\Delta t$, the updated Lagrangian referential is used. In this case, the configuration in instant t is used as the reference for the analysis, and structural system nonlinear dynamic response can be given by:

$$\mathbf{M}\ddot{\mathbf{U}} + \mathbf{C}\dot{\mathbf{U}} + \mathbf{F}_i(\mathbf{U}) = \lambda(t)\mathbf{F}_r \tag{18}$$

where **M** and **C** are the mass and damping matrices, respectively; **F***i* is the internal force vector; $\dot{\mathbf{U}}$, and $\ddot{\mathbf{U}}$, represent the displacement, velocity and acceleration vectors, respectively, of the structural system; $\mathbf{F}_r$ is the vector that defines the direction of the external excitation; and λestablishes the intensity of the load in a determined instant t.

According to Chopra (1995), the actions generated during an earthquake are not properly applied forces directly in the structure but inertial forces resulting from the structure itself moves. Thus, the acceleration throttle base or ground appears on the right side of the equation that governs the structural dynamic response as follows:

$$\mathbf{M}\ddot{\mathbf{U}} + \mathbf{C}\dot{\mathbf{U}} + \mathbf{F}_i = \ddot{\mathbf{U}}_g(t)\mathbf{M} \tag{19}$$

where $\ddot{\mathbf{U}}_g(t)$ is the acceleration of the ground, given by a scalar in a given time t.

In general, the structures behave non-linearly before reaching their limits of resistance. So the quest for a better representation of the structural behavior requires that the sources of nonlinearity are considered. As this paper are considered non-linear geometric effects and semi-rigid connections, rewrite Eq (19) as.:

$$\mathbf{M}\ddot{\mathbf{U}} + \mathbf{C}\dot{\mathbf{U}} + \mathbf{F}_i(\mathbf{U},\mathbf{P},\mathbf{S}_c) = \lambda(t)\mathbf{F}_r \tag{20}$$

where $\mathbf{F}_i$ is the vector obtained incrementally through formulations that consider the second order effects (represented here by the internal forces $\mathbf{P}$) and the semi-rigid connections (represented by parameter $\mathbf{S}_c$).

In this nonlinear structural study, the stiffness matrix is constantly updated to capture second order effects and the inelasticity of the material. An incremental-iterative solver is used which combines the methods of Newmark and Newton-Raphson (Silva, 2009; Batelo, 2014).

5 NUMERICAL APPLICATION

The semi-rigid connections can significantly alter the behavior of structures, so it is interesting to investigate their importance in seismic response to ensure that buildings have adequate strength and that the connections can prevent its collapse.

A four-bay five-story steel frame located in Shanghai, China, is investigated here, and its geometric configuration is similar to the structure shown in Fig. 6.

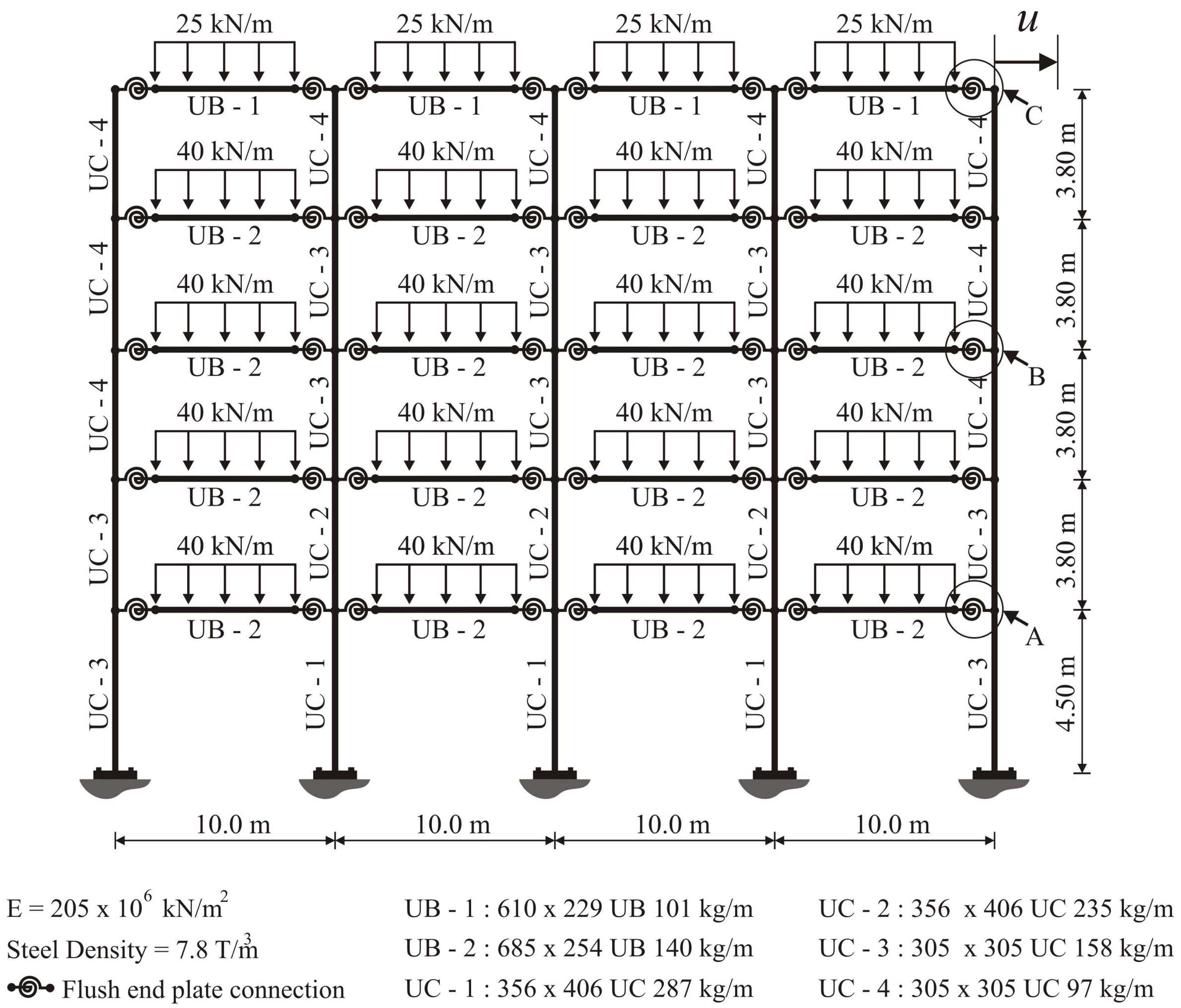

Figure 6. Geometric and material properties of four-bay five-story planar steel frame

The flush end plate beam-column connections are adopted and its behavior is represented by Richard Abbott model with the parameters: S_{cini} = 12336,86 *kNm/rad*, R_p = 112,97 *kNm/rad* , M_0= 96,03 *kNm* and n = *1,6* (Nguyen, 2010). Initially, only one element per member (beams and columns) are employed in the structure numerical modeling and gravitational loads are also included as additional lumped masses at the beams' nodes.

The frame is assumed to be subjected to the first ten seconds of the 1940 El Centro N-S earthquake component motion. This earthquake occurred in California, USA, on May 18, 1940. The first ten second records are shown in Fig. 7 and the peak ground acceleration observed was 0.31g.

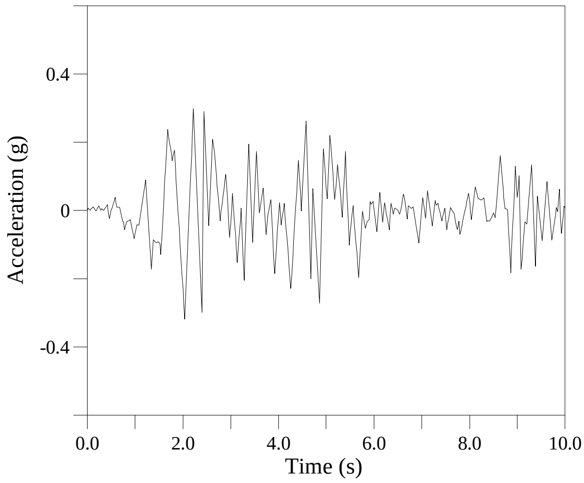

Figure 7. First ten seconds (N-S) El Centro ground motion acceleration (Thai and Kim, 2011)

The structure free vibration analysis considering the beam-column rigid connections was performed and the results are presented in Tab. 1 for the first two periods of vibration. See the reasonable approximation, even considering only one finite element per member, with the values found in the literature. In sequence, the first and second order elastic transient responses of the building with rigid connections, under this earthquake, were obtained and are presented in Fig. 8. Based on the lateral displacement at the top of the right-most column transient response, note the great influence of geometric nonlinearity in the response of the structure, which contribute significantly to the displacement amplification.

Table 1. First two natural periods of vibration (s) for the frame with rigid connections

Modes	Nguyen (2010)	Present Work
1	1.2282	1.1818
2	0.4345	0.4196

Table 2 presents the results for the structural system free vibration analysis when semi-rigid connection are adopted. Again, see the good approximation with the values found in the literature for the first two periods of vibration. Figure 9 shows the transient responses for the steel frame with these flexible connections, but considering only their linear behavior, where was assumed $S_c = S_{cini} = 12336{,}86$ *kNm/rad*. Once again, the influence of geometric nonlinear effects on the structure response is easily observed.

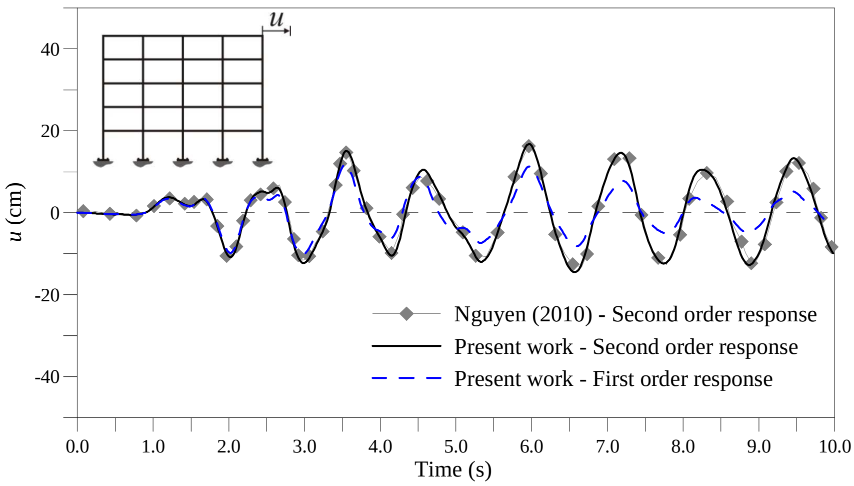

Figure 8. Horizontal displacement response at the structure roof level for rigid connections

Table 2. First two natural periods of vibration (s) for the frame with flexible connections

Modes	Nguyen (2010)	Present Work
1	2.700	2.623
2	0.777	0.773

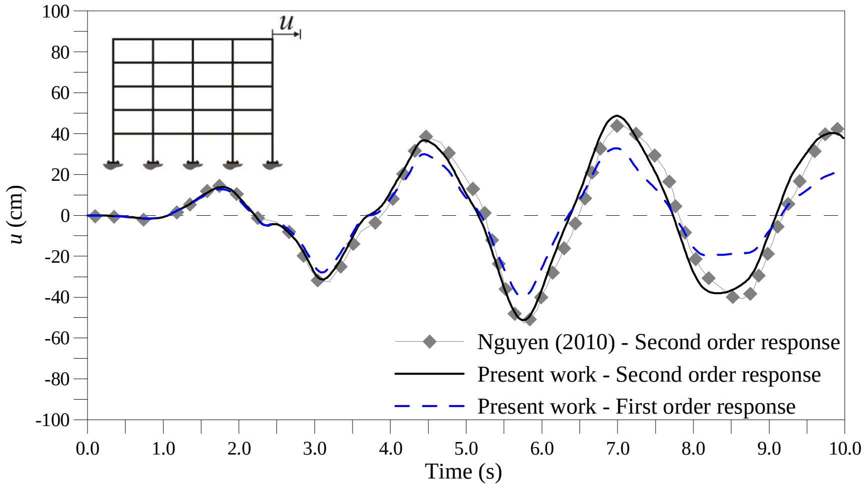

Figure 9. Horizontal displacement response at the structure roof level for semi-rigid connections with linear behavior

The variation of the planar steel frame natural frequencies with the beam-column connections flexibility is illustrated in Fig. 10. See that the connection flexibility has a significant influence on variation of the natural frequencies, particularly on the lower frequencies. This fact can be very important for frame structures seismic analysis, as the lower modes may have strong influence on buildings seismic response.

Now, Figure 11 shows the transient second order response of the steel frame with flexible connections, but considering its nonlinear behavior (Richard Abbott model). Again, attention is given to horizontal displacement variation at the structure roof. A small difference in nonlinear response observed with the respect to the literature results after six seconds have reduced when considering a better mesh refinement.

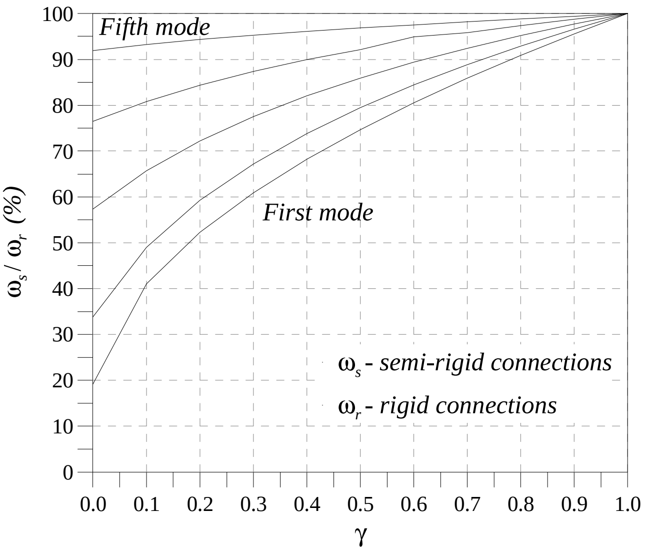

Figure 10. The influence of the beam-column connection flexibility on the natural frequencies

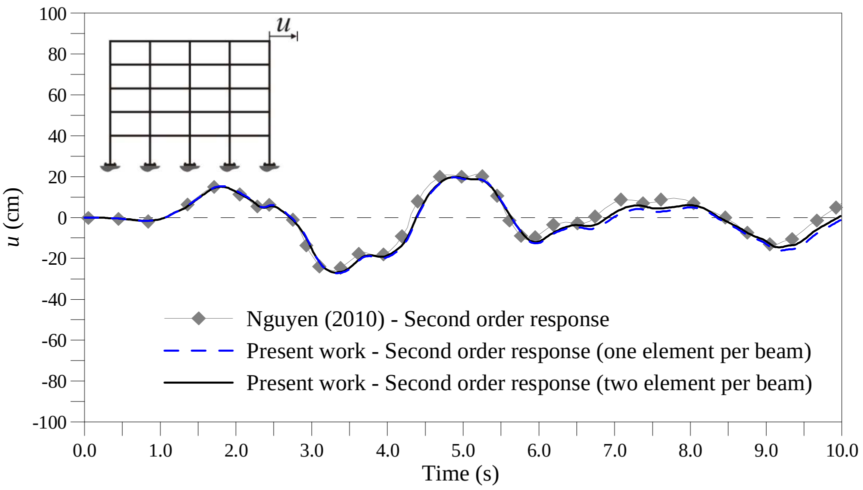

Figure 11. Horizontal displacement response at the structure roof level for semi-rigid connections with nonlinear behavior

The hysteretic moment-rotation loops at the semi-rigid joints A and C, as indicated in Fig. 6, are traced in Fig. 12a and 12b, respectively. Finally, the lateral displacement envelope of the planar steel frame is plotted in Fig. 13. See that the maximum deflection for the flush end plate joint case is approximately two times that for the rigid joint case. Also note that the backward deflection is much larger than the forward deflection due to permanent rotations formed at the connections of the flexibly connected frame.

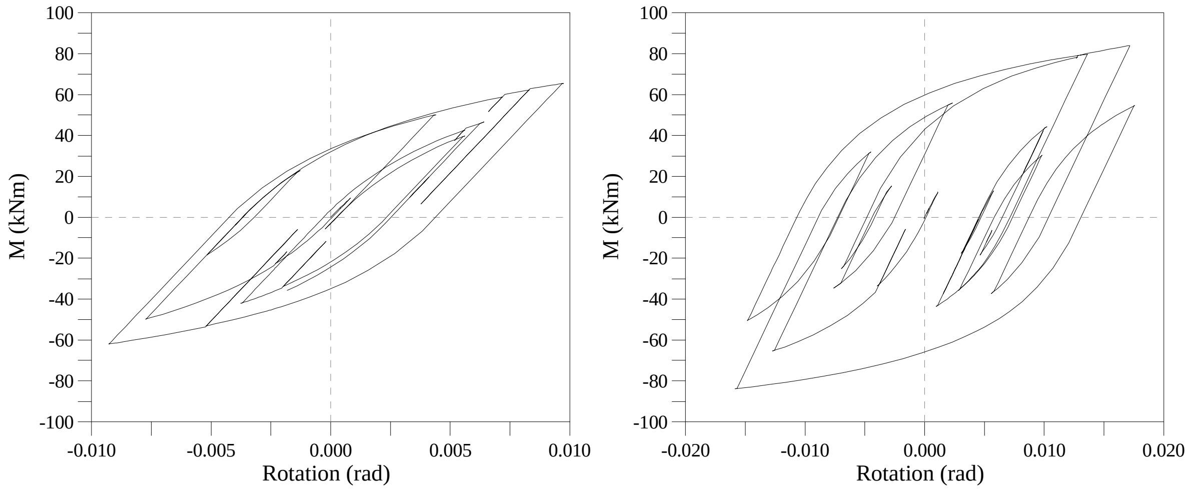

(a) Joint A (b) Joint C

Figure 12. Beam-column connection hysteretic behavior

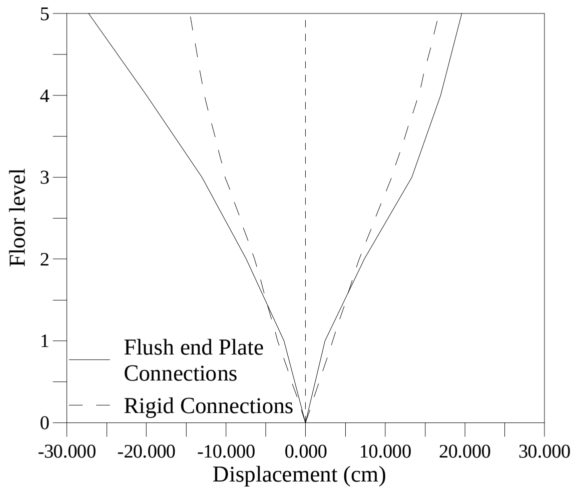

Figure 13. Lateral displacement envelope of the planar steel frame

6 FINAL REMARKS

From the study of the planar steel frame presented in the last section, it was found that the geometric nonlinear effect has significant influence on the displacements of the structure, especially after 6 seconds of excitation (Fig. 8). And it was also observed that the connection flexibility has significant influence on variation of the natural frequencies, particularly on the lower frequencies (Fig.10) and on the frame behavior.

In general, the results obtained here, mainly when considering the structure with flexible connections (linear and nonlinear behaviors), showed reasonable agreement with those from literature, even for the poor finite element mesh adopted on the modeling. This can demonstrate the applicability and precision of the numerical strategy proposed, whose transient nonlinear solver was based on an incremental-iterative strategy, which combines the methods of Newmark and Newton-Raphson.

It is worth informing that future authors' research should address the influence of the combined effects of geometric nonlinearity, steel inelasticity and semi-rigid connections on the nonlinear dynamic behavior of steel structures.

ACKNOWLEDGEMENTS

The authors are grateful to CAPES, CNPq (Federal Research Agencies), FAPEMIG (Minas Gerais Research Agency), PROPEC/Deciv/EM/UFOP and PROPP/UFOP for the financial support.

REFERENCES

ABNT - NBR 8800, 2008. Brazilian Association of Technical Standards. Project and Execution of Steel Buildings Structures, Rio de Janeiro, Brazil. (in Portuguese)

AISC, 2010.Specification for Structural Steel Buildings, American Institute of Steel Construction, ANSI/AISC 360-05, Chicago, IL.

Aristizabal-Ochoa, J. D., 2015. Stability of imperfect columns with nonlinear connections under eccentric axial loads including shear effects. *International Journal of Mechanical Sciences 90*.

Attarnejad, R., & Pirmoz, A., 2014. Nonlinear analysis of damped semi-rigid frames considering moment-shear interaction of connections. *International Journal of Mechanical Sciences 81*.

Batelo, E.A.P., 2014. *Advanced Dynamic Analysis of Steel Structures Under Extreme Loading*. Máster Dissertation, Deciv/EM/UFOP, Ouro Preto, MG, Brazil (in Portuguese).

Bernuzzi, C., Zandonini, R., & Zanon, P., 1996. Experimental analysis and modelling of semi-rigid steel joints under cyclic reversal loading. *Journal of Constructional Steel Research 38(2)*.

Calado, L., 2003. Non-linear cyclic model of top and seat with web angle for steel beam-to-column connections. *Engineering Structures 25*.

Chan, S.L., & Chui, P.P.T., 2000. *Non-linear Static and Cyclic Analysis of Steel Frames with Semi-Rigid Connections*. Elsevier, Oxford.

Chan, S.L., & Ho, G.W.M., 1994. Nonlinear vibration analysis of steel frames with semirigid connections. *Journal of Structural Engineering 120(4)*.

Chen, W.F., & Kim, S.E., 1997. *LRFD Steel Design using Advanced Analysis*, CRC Press, Boca Raton, Flórida.

A.K. Chopra, 1995. *Dynamics of Structures*, Prentice-Hall, Inc., New Jersey.

Cunningham, R., 1990. Some aspects of semi-rigid connections in structural steelwork. *The Structural Engineer 68(5).*

Eurocode 3, 2005. Design of Steel Structures. Part 1.8: Design of Joints. European Committee for Standardization (CEN) Brussels, Belgium.

Galvão, A.S., Silva, A.R.D., Silveira, R.A.M., & Gonçalves, P.B., 2010. Nonlinear dynamic and instability of slender frames with semi-rigid connection. *International Journal of Mechanical Sciences 52*.

Kishi, N. , Komuro, M., & Chen, W.F., 2004. Four-parameter power model for M–θ curves of end-plate connections. *In: ECCS/AISC workshop connections in steel structures V: Innovative steel connections*.

Kishi, N., & Chen, W.F., 1986. Data Base of Steel Beam-to-column Connections. Structural Engineering Report No. CE-STR-93-15, School of Civil Engineering, Purdue Univ., West Lafayette, IN.

Lima, S.S., & Santos, S.H.C., 2008. *Análise Dinâmica de Estruturas*. Editora Ciência Moderna Ltda, Rio de Janeiro.

Lui, E.M., & Lopes, A., 1997. Dynamic analysis and response of semirigid frames. *Engineering Structures, 19(8).*

Nguyen, P-C., 2010. *Nonlinear Analysis of Planar Semi-Rigid Steel Frames subjected to Earthquakes using PlasticZone Method*. Master Dissertation, Hồ Chí Minh, Vietnam, (in Vietnamese.

Nguyen, P-C., & Kim, S-E., 2011. Nonlinear elastic dynamic of space steel frames with semi-rigid connections. *International Journal Constructional Steel Research 84.*

R.M. Richard, & B.J. Abbott, 1975. Versatile elastic-plastic stress-strain formula. *Journal of the Engineering Mechanics Division 101(4).*

Silva, A.R.D., 2009. *Computational System for Static and Dynamic Advanced Analysis of Steel Frames*, Ph.D. thesis, PROPEC/Deciv/UFOP, Ouro Preto/MG, Brazil, (in Portuguese).

Shi, G., Shi Y., & Wang Y., 2007. *Behavior of end-plate moment connection under earthquake loading. Engineering Structures*, 29.

Sophianopoulos, D.S., 2003. The effect of joint flexibility on the free elastic vibration characteristics of steel plane frames. *Journal of Constructional Steel Research 59* .

Thai, H.-T., & Kim, S. E. 2011. Second-order inelastic dynamic analysis of steel frames using fiber hinge method. *Journal of Constr. Steel Research*, Vol. 67..

Valipour, H.R., & Bradford, M., 2012. An efficient compound-element for potential progressive collapse analysis of steel frames with semi-rigid connections. *Finite Elements in Analysis and Design, 60*.

Vimonsatit, V., Tangaramvong, & S. F., Tin-Loi, 2012. Second order elastoplastic analysis of semirigid steel frames under cyclic loading. *Engineering Structures 65*.

Xu, Y.L., & Zhang, W.S., 2001. Modal analysis and seismic response of steel frames with connection dampers. *Engineering Structures 23*.